arXiv:1207.7066v1 [cond-mat.str-el] 29 Jul 2012

Incoherent Soliton Excitations and Spin-Charge Separation in Blue Bronze

Daixiang Mou,[1] R. M. Konik,[2] A. M. Tsvelik*,[2] I. Zaliznyak,[2] and Xingjiang Zhou*[1]
[1] *National Laboratory for Superconductivity, Beijing National Laboratory for Condensed Matter Physics,*
Institute of Physics, Chinese Academy of Sciences, Beijing 100190, China
[2] *CMPMS Dept., Brookhaven National Laboratory, Upton, NY 11973-5000, USA*[2]

(Dated: August 1, 2012)

We present and analyze high resolution angle resolved photoemission (ARPES) data for $K_{0.3}MoO_3$ (blue bronze). The observed Fermi surface, with two sheets that are one dimensional in nature, is consistent with a ladder material with only weak inter-ladder coupling. The marked broadening of the ARPES lineshape, a significant fraction of an eV, can be interpreted in terms of the intra-ladder interaction between the bonding and antibonding bands of the ladder that leads to spin-charge separation. The interaction also gives rise to asymmetry in the dispersions seen to the left and the right of a given Fermi point. With improved energy resolution, a high energy feature is revealed for the first time in the photoemission spectra near the Fermi momentum. We believe this new feature is indicative of a higher energy bound state of soliton excitations on a ladder.

PACS numbers: 74.81.Fa, 74.90.+n

Systems of two coupled chains can be viewed as a first step in crossing over from one dimension, with all of its exotic physics of Luttinger liquid induced spin-charge separation, to higher dimensions. How these properties are transformed in the course of this crossover is why such systems (also called ladders) have been intensely studied by theorists. While theoretical progress on this problem has been considerable, with work in predicting rich excitation spectra, dynamical generation of spectral gaps, existence of preformed pairs [1–15], the progress on the experimental side has been slower both due to limited numbers of materials with a suitable structure and limited experimental accuracy.

$K_{0.3}MoO_3$ (blue bronze) is a quasi-one-dimensional (1D) material consisting of an array of weakly coupled pairs of conducting ladders [16]. Band structure calculations predict that the chemical potential is crossed by two slightly warped bands corresponding to 3/4-filling [17, 18]. These bands, arising from the uncoupled ladders, are composed of bonding (B) and anti-bonding (AB) bands with Fermi wave vectors K_{FB} and K_{FAB} respectively. The Fermi surface nesting leads to charge density wave (CDW) formation with a wave vector along the chains equal to $K_{FB} + K_{FAB}$. A three-dimensional (3D) phase transition into a charge-ordered insulating phase takes place at a temperature $T_{CDW} = 180K$ [19, 20] even though the magnetic susceptibility starts to decrease well above the transition, experiencing a one-third drop in the interval between 700K and 180K [19]. The corresponding activation gap is estimated to be 30-40 meV [21]. Although the CDW related properties are well studied in blue bronze [22], its characteristics as a ladder material are much less well understood.

In this paper we report the results of high resolution angle-resolved photoemission (ARPES) measurements of the ladder material $K_{0.3}MoO_3$. With much improved instrumental resolution, we resolve for the first time two features in the measured photoemission spectra. These two features are broad peaks in regions of the Brillouin zone near the Fermi vector, dispersing through energies of a significant fraction of an eV. We interpret them as ladder excitations originating from the same interaction that underpins the three dimensional charge order existing in this material at low temperatures. The breadth of these peaks arises from the presence of gapless charge excitations (holons) and gapful spin solitons (spinons) with markedly different velocities. Assuming that the electron-lattice interaction plays a secondary role and the physics is electron-driven, we obtain a good description of the higher energy portion of the spectral function with two SU(2) Thirring models.

The $K_{0.3}MoO_3$ single crystals were grown by an electrolytic reduction method [23]. High resolution angle-resolved photoemission measurements were carried out with a Scienta R4000 electron energy analyzer [24]. For the band structure measurements and Fermi surface mapping (Fig. 1), we used a helium discharge lamp as the light source with a photon energy of $h\nu$ =21.218 eV. The overall energy resolution was set at 10 meV and the angular resolution was 0.3°, corresponding to a momentum resolution of 0.0091 $Å^{-1}$ at the photon energy of 21.218 eV. For the high-precision ARPES measurements (Fig. 2 and Fig. 3), a vacuum ultra-violet (VUV) laser with a photon energy $h\nu$=6.994 eV was used as a light source. The energy resolution used in this case was 1 meV. The angular resolution is 0.3°, corresponding to a momentum resolution of 0.004 A^{-1} at the photon energy of 6.994 eV. The Fermi level is referenced from measuring a clean polycrystalline gold that is electrically connected to the sample. The crystal was cleaved *in situ* and measured in vacuum with a base pressure better than 5×10^{-11} Torr.

Fig. 1a shows the bare Fermi surface (FS). The data for this figure are collected at 80K. The FS is open and consists of weakly warped sheets, indicating a weak inter-ladder coupling. Based on the the warping of the extracted Fermi momentum (blue dots in Fig. 1a), one can estimate the coupling to be $t_\perp \approx 100$ meV . Fig 1b shows the band structure measured along the Γ-Y cut at 80 K.

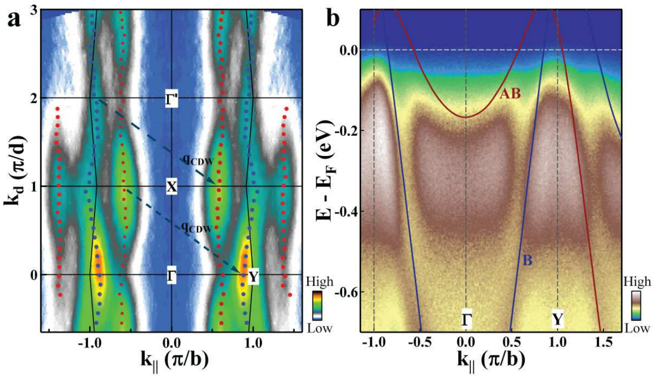

FIG. 1: a) The bare Fermi surface of $K_{0.3}MoO_3$ extracted from the measurements. Data are symmetrized with respect to the $k_{||}$=0 line. Blue and red dots stand for the extracted Fermi momentum along the Fermi surface sheets. The CDW vectors are marked by the dashed arrows. b) The measured band structure along Γ-Y (k_d = 0) showing two bands, the bonding band (B) and the anti-bonding band (AB), crossing the Fermi level. The solid lines mark bands predicted from band structure calculations [18].

At energies less than 1eV we can clearly distinguish two bands (B and AB). The non-interacting bands cross the chemical potential at 0.97 π/b, 0.6 π/b, -0.55 π/b and -0.96 π/b, consistent with the band structure calculations in Ref. 18 and previous ARPES measurements [25, 26]. The Fermi surface nesting vector is thus estimated to be ≈ 1.52 π/b, also in good agreement with the measured CDW vector [27, 28].

In Fig. 2 and Fig. 3, we present high resolution laser ARPES data for the band structure along the ladder at $k_d = 0$. Due to the effects of matrix elements, the B band is more clearly visible than the AB band (Fig. 2a). Its electronic structure exhibits two features clearly distinguished in the second derivative image (Fig. 2b), seen as excitation branches near K_{FB}. The lower binding-energy branch was observed in earlier ARPES measurements [25, 26], while the second higher energy branch has not hitherto been seen. The lower branch, starting at ≈ 60 meV below E_F, reaches in energy as low as -0.8 eV as $k_{||}$ varies from π/b to 0.4 π/b (red circles in Fig. 2b). The second branch with a lower spectral weight starts at ≈ 150 meV, remains distinct until roughly ≈ -200 meV, and then merges with the first branch (blue circles in Fig. 2b). The two branches gradually become indistinguishable when the temperature increases (Fig. 3(a - e)). At high temperature (240K), only one broad hump is observed (Fig. 3e). A further feature not previously seen but that we observe is the left-right asymmetry of the low energy branch: the slope of the band on the right side of the Fermi momentum ($k_{||} > K_{FB}$) $v_R \approx 0.96$ eV$\mathring{A}$ is smaller than that on the left side ($k_{||} < K_{FB}$): $v_L \approx 4.42$ eV$\mathring{A}$. These roughly correspond to the expected velocities of the B and AB bands [18]. We will argue that both the presence of two excitation branches and the asymmetry of their dispersion can be explained in terms of one-dimensional intra-ladder interactions.

There are two standard approaches to investigate quasi-1D systems. One can take the transverse tunneling into account on the first step and treat the interactions via a perturbative renormalization group and mean field. This approach predicts all sorts of Fermi surface instabilities and related 3D phase transitions (CDW, superconductivity, etc.), but has difficulty in describing strong fluctuations and all related effects such as incoherence of the excitations [29]. An alternative approach is to consider the 1D subsystem (in this case, a ladder) with all of its interactions as a basis for calculations, use the powerful non-perturbative techniques available in one dimension, and then treat the interladder interactions as a perturbation [30–32]. The strong precursor effects observed such as the drop in the magnetic susceptibility [19] and the absence of Fermi crossing in a wide temperature range above the CDW transition (Fig. 3) suggest that the second approach better captures the physics of the material in question. This point of view is further supported by our ARPES measurements showing a strongly incoherent single particle spectral function (Fig. 2c).

The previous attempts to explain the broad ARPES

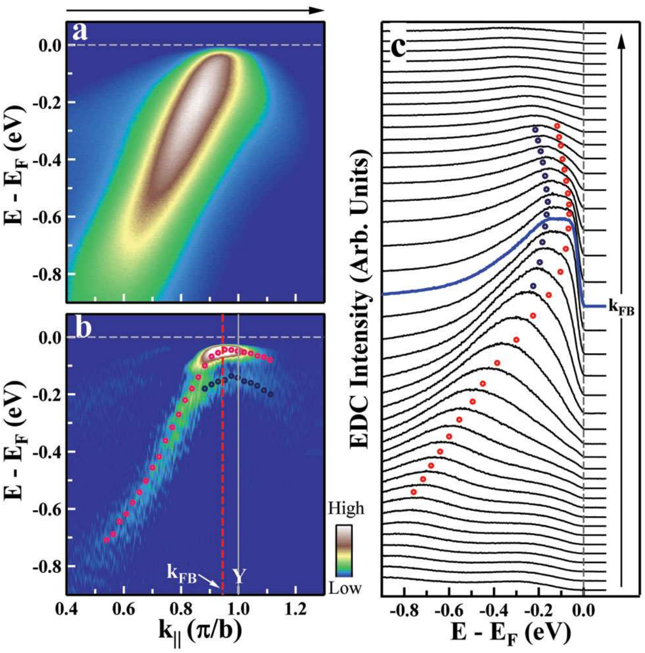

FIG. 2: a) High resolution measurement of the band structure along Γ-Y momentum cut with 1 meV energy resolution. Due to matrix element effects, only the B band is clearly observed. b) Second derivative with respect to energy of the data in (a). Two structures around k_{FB}, corresponding to incoherent soliton and bound state (see text), are clearly seen. c) The corresponding photoemission spectra (EDCs). Two features are clearly resolved for the spectra near the Fermi momentum k_{FB}. Red (blue) circles mark in b) and c) mark the dispersion of the soliton and the bound state.

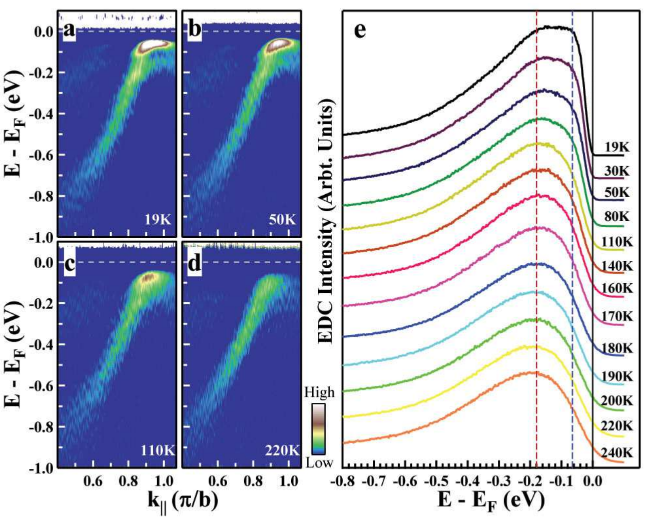

FIG. 3: a) - d) EDC second derivative images of the B band along Γ-Y momentum cut at different temperatures. The data are divided by the Fermi-Dirac function. e) Extracted K$_{FB}$ EDCs at different temperatures. Two energy scales of incoherent soliton and bound state are marked by blue and red dashed lines, respectively.

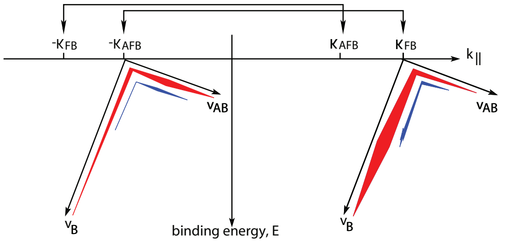

FIG. 4: Schematic of interaction between pairs of Fermi points, $(K_{FB}, -K_{FAB})$ and $(K_{FAB}, -K_{FB})$. For the first pair we show the asymmetry in the dispersion on either side of these two Fermi points. The width of the red stripe indicates the expected intensity of the dispersing incoherent soliton (gapped spinon and gapless holon) observed by ARPES. The blue stripe marks the corresponding intensity of a two particle continua composed in part by a dispersing bound state. The intensities at $-K_{FAB}$ are shown as lower because of matrix element effects.

spectrum have been based on small polaron theory [25, 33]. However, the shear size of the gaps and the wide energy range of the incoherence tails, spreading into a significant fraction of an eV, suggests that these features have an electronic origin. This incoherence cannot be explained in terms of the standard band structure theory even modified with 3D Fermi liquid corrections. However, there are non-perturbative calculations for the single electron spectral functions which we will argue provide a qualitative fit to the data.

In all 1D theories the incoherence originates from quantum fluctuations of the gapless holon mode (in the case at hand it is the mode that describes the dynamics of the charge density wave). The spectrum of this mode at low energies has a linear dispersion, i.e., $\omega = v_c|k|$. Since the CDW instability occurs at the wave vector $k_{FB} + k_{FAB}$, both bands are involved in creation of the order parameter. However, as is clearly seen on Fig. 2b, these bands have very different Fermi velocities v_{FB} and v_{FAB} - a feature that is not present in standard theories of 2-leg ladders where this difference is neglected. This velocity difference precludes the emergence of an SO(6) symmetry, the latter effect being one of the most interesting predictions of the low energy theory of ladders [2, 3]. However we will argue that a remnant of this symmetry remains in the form of an electron-hole bound state.

Below we describe a low energy theory which is chosen in such a way that (i) it maximizes the fluctuations leading to the observed incoherency of the ARPES lineshapes and (ii) it gives rise to a zero temperature CDW instability at $k_{FB} + k_{FAB}$ which, in the presence of 3D coupling, is shifted to finite temperatures. Since the spectral gaps are much smaller than the bandwidth, it is reasonable to linearize the dispersion close to the Fermi points by introducing slowly varying right- and left-moving components of the fermionic fields

$$\psi_{j\sigma} = \mathrm{e}^{-ik_{Fj}x}\psi_{Rj\sigma} + \mathrm{e}^{ik_{Fj}x}\psi_{Lj\sigma}, \quad j = B, AB. \qquad (1)$$

Because of the different Fermi velocities in the bonding and anti-bonding bands, we expect the theory will not have a symmetry higher then U(1)×SU(2). Moreover, we expect the strongest interaction to occur between the bonding and anti-bonding bands, foreshadowing the rise of the observed 3D CDW order. To this end we consider a model where the fermions at K_{FB} interact with the fermions at $-K_{FAB}$ and similarly those at $-K_{FB}$ interact with fermions at K_{FAB}. This leads us to describe the system as two decoupled 1D theories, $H = H_1 + H_2$:

$$H_1 = \int dx\Big(-iv_{FB}\psi^\dagger_{RB\sigma}\partial_x\psi_{RB\sigma}$$
$$+iv_{FAB}\psi^\dagger_{LAB\sigma}\partial_x\psi_{LAB\sigma} + g_0\rho_{RB}\rho_{LAB} + gJ^a_{RB}J^a_{LAB}\Big);$$
$$\rho_{R,b} = \psi^\dagger_{RB\sigma}\psi_{RB\sigma}, \quad J^a_{RB} = \psi^\dagger_{RB\sigma}\tau^a_{\sigma\sigma'}\psi_{RB\sigma'}; \qquad (2)$$

with $H_2 = H_1(AB \leftrightarrow B)$ and where τ^a are Pauli matrices. The coupling constant g is equal to the $K_{FB} + K_{FAB}$ Fourier component of the renormalized Coulomb interaction. We take it to be positive, corresponding to an attractive interaction that is necessary for CDW formation. The spectrum of both H_1 and H_2 consists of a gapless, spinless holon mode and a chargeless spinon mode with gap $\Delta \sim W(g/v)^{1/2}\exp(-\pi v/g)$ where $v = (v_{FB} + v_{FAB})/2$. The other coupling g_0 comes from forward scattering, the $k = 0$ component of the Coulomb interaction. Both g and g_0 are associated with a renormalization of the spinon and holon velocities.

The spectral function corresponding to this theory can be obtained from the one for the case of equal Fermi velocities v, studied in [30] by a simple Galilean transformation: $t' = t, \quad x' = t\Delta v + x, \quad \Delta v = (v_{FB} - v_{FAB})/2$.

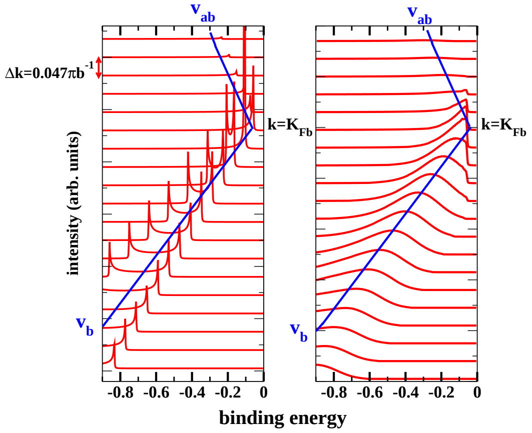

FIG. 5: EDCs for the B band for k-vectors ranging from $k = 0.4\pi b^{-1}$ to $k = 1.3\pi b^{-1}$: a) before averaging for differential surface doping; b) after averaging with a Gaussian of width $0.07\pi b^{-1}$.

We so obtain:

$$\begin{aligned}\langle T(\psi_\sigma(0,0)\psi_\sigma^\dagger(0,0)\rangle &= \\ &\sum_{j=B,AB}\left(\mathrm{e}^{ik_{Fj}x}G_{Rj}(\tau,-x)+\mathrm{e}^{-ik_{Fj}x}G_{Lj}(\tau,x)\right),\\ G_{LAB}(\tau,x) &= \frac{Z}{\sqrt{(v_{s+}\tau+ix)(v_{c+}\tau+ix)}}\\ &\times\exp\Big[-\frac{\Delta}{v_c}\sqrt{(v_{c+}\tau+ix)(v_{c-}\tau-ix)}\Big],\end{aligned}\qquad(3)$$

where $Z \sim 1$, $v_{c,s,\pm} = v_{c,s} \pm \Delta v$, and $G_{LB}(\tau,x) = G_{LAB}(\tau,x,v_{AB} \leftrightarrow v_B)$. The corresponding retarded Green function in Fourier space is

$$\begin{aligned}G_{LAB}(\omega,k) &= Z\frac{2}{1+\alpha}F(\omega+k\Delta v,k);\\ F(\omega,k) &= \frac{\tilde{\omega}-v_ck}{\Delta^2+v_c^2k^2-\tilde{\omega}^2}\Big[\big(\Delta+\sqrt{\Delta^2+v_c^2k^2-\tilde{\omega}^2}\big)^2\\ &\quad-\frac{1-\alpha}{1+\alpha}(\tilde{\omega}-v_ck)^2\Big]^{-1/2},\end{aligned}\qquad(4)$$

where $\alpha = v_s/v_c$ and $\tilde{\omega} = \omega + i\delta$.

The most notable prediction of this theory is that the spectral features at any Fermi point ($\pm K_{FB}, \pm K_{FAB}$) will appear to disperse with different velocities to its right and left. This is illustrated schematically in Fig. 4 for the pair of Fermi points K_{FB} and $-K_{FAB}$. We also see the observed asymmetry on the spectrum in Fig. 5 where we plot the expected line shapes for a set of EDCs for different k's in the vicinity of K_{FB}: for $k < K_{FB}$ the spectral weight disperses with velocity v_{FB} while for $k > K_{FB}$ the spectral weight, while much reduced, disperses with velocity v_{FAB}.

In Fig. 5a we see how spin-charge separation leads to broadened features in the ARPES lineshape giving rise to two singularities in the spectral weight at an upper and a lower energy that disperse with different velocities (the spin and charge velocities) as k moves away from a Fermi point. However, different spin and charge velocities alone cannot explain the broad linewidths observed. We believe a part of the broadening of the lineshapes arises from $K_{0.3}MoO_3$ being a poor conductor. Poor conductivity will lead to ladders in different regions on the surface of the sample to be at different dopings. This in turn will lead to a spatial dependence of K_{FB} and K_{FAB}. In fact, such dependence was observed in a scanning tunneling microscopy study of a sister blue bronze $Rb_{0.3}MoO_3$ [34], where K_F was found to vary across the surface from about $0.65b^*$ to about $0.80b^*$ ($b^* = 2\pi/b$). This could also explain the significant $0.1\mathring{A}^{-1}$ breadth of the momentum distribution curve at E_F in $K_{0.3}MoO_3$ reported in Fig. 5(c) of [25]. To account for this effect we convolve the lineshapes with a Gaussian weight function of width $= 0.07\pi b^{-1}$. We do this on the r.h.s. of Fig. 5 where we observe a considerable increase in broadening. The ARPES measurements on the 1D Mott-Hubbard insulator, $SrCuO_2$, considered the best evidence for spin-charge separation, also yield broad peaks much broader than the corresponding theoretical prediction (see Fig. 3 in [36]). We thus believe that such broadening is an inherent feature of ARPES measurements on insulating systems originating, again, from some inhomogeneity or disorder present in the samples.

We have so far ignored interactions between fermions living at $K_{FB}, -K_{FAB}$ and $-K_{FB}, K_{FAB}$. However, such interactions are present even though they are weaker than those responsible for the 3D CDW order. In a ladder system with equal velocities in the bonding and anti-bonding bands, the theory governing the low energy response has a dynamically generated SO(6) symmetry, and so predicts that there will be a bound state of the spin degrees of freedom of the electrons [3]. This bound state contributes to a response above the gap, Δ, of the single particle spectral function. In a purely SO(6) theory this response leads to a feature in the spectral function at an energy $\omega = (1+\sqrt{2})\Delta$ for $k = K_{FB}, K_{FAB}$. While in a theory with broken SO(6) symmetry (i.e., $v_B \neq v_{AB}$) we cannot predict where exactly this threshold will occur, we can say that this bound state will survive even in the presence of symmetry breaking, a consequence of the bound state having significant binding energy making it stable to perturbations. This bound state offers an explanation for the second peak observed in Fig. 2b at an energy roughly twice that of the gap.

In conclusion, we have presented high resolution ARPES data for the CDW material $K_{0.3}MoO_3$. We have argued that the features in the ARPES lineshapes, including incoherent broadening and asymmetric dispersions from the same Fermi point, can be understood primarily as arising from strong correlations in one dimension.

Authors are grateful for constructive conversations with Alan Tennant as well as useful comments by both P. D. Johnson and by F.H.L. Essler. XJZ thanks financial support from the MOST of China (973 program No: 2011CB921703). The work was also supported by the

US DOE under contract number DE-AC02-98 CH 10886 (RMK, AMT, IZ). RMK and AMT also thank the Galileo Galilei Institute for Theoretical Physics and the INFN for kind hospitality and support during the completion of this work.

[1] M. Fabrizio, Phys. Rev. B **48**, 15838 (1993).

[2] L. Balents and M. P. A. Fisher, Phys. Rev. B**53**, 12133 (1996); H. H. Lin, L. Balents and M. P. A. Fisher, Phys. Rev. B**58**, 1794 (1998).

[3] H.J. Schulz, Phys. Rev. B**53**, R2959 (1996); ibid, cond-mat/9808167.

[4] D. V. Khveshchenko and T. M. Rice, Phys. Rev. B **50**, 252 (1994).

[5] R. Konik, F. Lesage, A. W. W. Ludwig, and H. Saleur, Phys. Rev. B **61**, 4983 (2000); R. Konik and A. W. W. Ludwig, Phys. Rev. B **64**, 155112 (2001); R. Konik, F. Lesage, A. W. W. Ludwig, and H. Saleur, Phys. Rev. B **61**, 4983 (2002).

[6] C. M. Varma and A. Zawadowski, Phys. Rev. B **32**, 7399 (1985).

[7] D. Controzzi and A. M. Tsvelik, Phys. Rev. B **72**, 035110 (2005).

[8] C. Lee, P. Azaria, and E. Boulat, Phys. Rev. B **69**, 155109 (2004).

[9] M. Tsuchiizu and A. Furusaki, Phys. Rev. B **66**, 245106 (2002).

[10] C. Wu, W. V. Liu, and E. Fradkin, Phys. Rev. B **68**, 115104 (2004).

[11] R. M. Noack, S. R. White, and D. J. Scalapino, Phys. Rev. Lett. **73**, 882 (1994); R. M. Noack, S. R. White, and D. J. Scalapino, Physica C 270, **281** (1996); R. M. Noack, M. G. Zacher, H. Endres, and W. Hanke, cond-mat/9808020.

[12] E. Jeckelmann, D. J. Scalapino, and S. R. White, Phys. Rev. B **58**, 9492 (1998).

[13] Z. Weihong, J. Oitmaa, C. J. Hamer, and R. J. Bursill, J. Phys.:Condens. Matter **13**, 433 (2001).

[14] D. Poilblanc, E. Orignac, S. R. White, and S. Capponi, Phys. Rev. B **69** , 220406R (2004).

[15] A. M. Tsvelik, Phys. Rev. B**83**, 104405 (2011).

[16] J. Graham and A. D. Wadsley, Acta. Crystallogr. **20**, 93 (1966).

[17] E. Canadell and M.-H. Whangbo, Chem. Rev. **91**, 965 (1991).

[18] J.-L. Mozos, P. Ordejón, and E. Canadell, Phys. Rev. B **65**, 233105 (2002).

[19] D. C. Johnston, Phys. Rev. Lett. **52**, 2049 (1984).

[20] R. S. Kwok, G. Gruner and S. E. Brown, Phys. Rev. Lett. **65**, 365 (1990).

[21] W. Brutting, P. H. Nguyen, W. Riess and G. Paasch, Phys. Rev. B **51**, 9533 (1995).

[22] M. Greenblatt, Chem. Rev. **91**, 965 (1988).

[23] C. Li, *et al.*, J. Cryst. Growth, **285**, 81 (2005).

[24] G. D. Liu *et.al.*, Rev. Sci. Instrum. **79**, 023105 (2008).

[25] L. Perfetti *el al.*, Phys. Rev. B **66**, 075107 (2002).

[26] H. Ando *et.al.*, J. Phys.:Condens. Matter **17**, 4935 (2005).

[27] M. Sato *et al.*, J. Phys. C: Solid State Phys. **18**, 2603 (1985).

[28] J. P. Pouget *et al.*, J. Phys. Lett. **44**, L113 (1983).

[29] C. Boubonnais and L. G. Caron, Int. J. Mod. Phys. **5**, 1033 (1991).

[30] F. H. L. Essler and A. M. Tsvelik, Phys. Rev. B **65**, 115117 (2002).

[31] F. H. L. Essler and A. M. Tsvelik, Phys. Rev. B **71**, 195116 (2005).

[32] R. M. Konik, T. M. Rice and A. M. Tsvelik, Phys. Rev. Lett. **96**, 86407 (2006).

[33] O. Röscha and O. Gunnarsson, Eur. Phys. J. B **43**, 11 (2005).

[34] C. Brun *et.al.*, J. Phys.: Conf. Ser. **61**, 140 (2007).

[35] F. H. L. Essler and A. M. Tsvelik, Phys. Rev. Lett. **90**, 126401 (2003).

[36] B. J. Kim *et. al.*, Nature Physics **2**, 397 (2006).